pubs.acs.org/acschemicalbiology

Articles

Clinical Antiviral Drug Arbidol Inhibits Infection by SARS-CoV-2 and Variants through Direct Binding to the Spike Protein

Anton Shuster,[§] Dany Pechalrieu,[§] Cody B Jackson, Daniel Abegg, Hyeryun Choe, and Alexander Adibekian*

Cite This: https://doi.org/10.1021/acschembio.1c00756

Read Online

ACCESS | Metrics & More | Article Recommendations | Supporting Information

ABSTRACT: Arbidol (ARB) is a broad-spectrum antiviral drug approved in Russia and China for the treatment of influenza. ARB was tested in patients as a drug candidate for the treatment at the early onset of COVID-19 caused by the novel severe acute respiratory syndrome coronavirus 2 (SARS-CoV-2). Despite promising clinical results and multiple ongoing trials, preclinical data are lacking and the molecular mechanism of action of ARB against SARS-CoV-2 remains unknown. Here, we demonstrate that ARB binds to the spike viral fusion glycoprotein of the SARS-CoV-2 Wuhan strain as well as its more virulent variants from the United Kingdom (strain B.1.1.7) and South Africa (strain B.1.351). We pinpoint the ARB binding site on the S protein to the S2 membrane fusion domain and use an infection assay with Moloney murine leukemia virus (MLV) pseudoviruses (PVs) pseudotyped with the S proteins of the Wuhan strain and the new variants to show that this interaction is sufficient for the viral cell entry inhibition by ARB. Finally, our experiments reveal that the ARB interaction leads to a significant destabilization and eventual lysosomal degradation of the S protein in cells. Collectively, our results identify ARB as the first clinically approved small molecule drug binder of the SARS-CoV-2 S protein and place ARB among the more promising drug candidates for COVID-19.

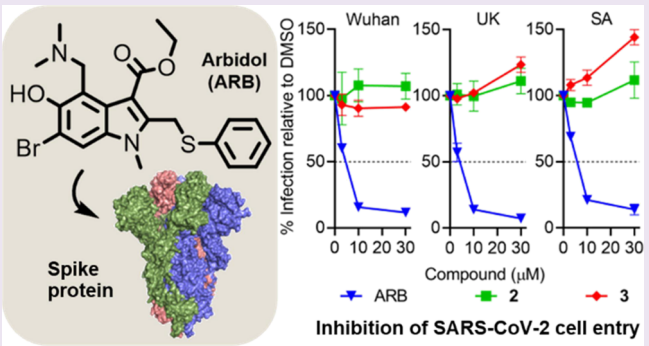

INTRODUCTION

The severe acute respiratory syndrome coronavirus 2 (SARS-CoV-2), a newly identified human betacoronavirus, is the cause of the ongoing global pandemic named COVID-19.[1−3] As of February 2021, the World Health Organization reported over 100 million cases of COVID-19 in over 200 countries, leading to over 2 million deaths worldwide.[4] The ever-increasing number of daily cases, fatality rates, scarcity of specific treatments, and the emergence of new mutant variants of SARS-CoV-2 continue to have a deep impact on daily life and the global economy and place COVID-19 pandemic among the worst recent humanitarian disasters.

Remdesivir, a broad-spectrum nucleotide analogue inhibitor of viral RNA-dependent RNA polymerases developed against Ebola, is so far the only FDA-approved small molecule COVID-19 therapeutic.[5] A phase III study showed shortened time to recovery in remdesivir-treated COVID-19 patients, but the mortality rates remain high.[6] Several monoclonal antibody drugs developed against the spike protein of SARS-CoV-2 were recently granted emergency use authorization, but the available data are insufficient to confirm the efficacy, while their prescription is limited to nonhospitalized patients with mild cases.[7−9] Several COVID-19 vaccines were made available worldwide in the past year, but the supply is limited, and vaccine distrust and hesitancy in the population remain a fundamental problem.[10] Most importantly, the recent emergence and rapid spread of more virulent mutant forms of SARS-CoV-2 add to the existing healthcare threat.[11,12] The spike protein mutations in these variants possibly compromise the efficacy of the approved COVID-19 therapeutics and vaccines, thus urging the need for new efficacious therapeutics to counter them.[13−15]

Unprecedented time pressure made repurposing of already approved therapeutics toward COVID-19[16−18] a particularly attractive and likely the only viable option. Over 200 ongoing clinical trials are mainly focused on antiviral, antimalarial, anti-inflammatory drugs and immunomodulators.[19] Among these, 11 trials explore monotherapy and various combinations of a broad-spectrum antiviral drug Arbidol (ARB, umifenovir) that was approved as an influenza medication in Russia in 1993 and in China in 2006 and is available over-the-counter.[20] Outside

Received: September 28, 2021
Accepted: November 9, 2021

of its main indication, ARB demonstrated efficacy against various other human viruses.[21−26] ARB has also been successfully evaluated for the treatment of SARS-CoV, the previous strain of human coronavirus responsible for the 2003 SARS epidemic.[27−29]

At the onset of the COVID-19 pandemic in China, ARB was directly employed in clinics as a test treatment. Clinics in Wuhan prescribed ARB as part of the first-line treatment for patients displaying SARS-CoV-2-related dyspnea, hypoxia, and viral pneumonia.[30] A clinical study attested improvement in computed tomography (CT) chest scans in adult COVID-19 patients who received ARB and lopinavir/ritonavir (LPV/r) compared to the LPV/r group only.[31] ARB monotherapy was later described as potentially superior to LPV/r alone based on the reduced viral load and shorter positive RNA test duration in the ARB patient group.[32] Decreased mortality and faster discharge rates were observed upon ARB administration to COVID-19-diagnosed patients at the Union Hospital in Wuhan.[33] ARB also efficiently inhibited the SARS-CoV-2 infection in Vero E6 cells with 4.11 μM EC_{50} and outperformed benchmark antivirals baloxavir, laninamivir, oseltamivir, peramivir, and zanamivir.[34] However, the direct molecular mechanism of ARB's activity against SARS-CoV-2 remains unknown, and no target identification studies have been reported to date. A detailed mechanistic understanding of ARB's activity is crucial to further evaluate its potential as a COVID-19 therapeutic and to enable the development of similarly acting drugs.

In this study, we make use of an ARB-based photoaffinity probe to elucidate the mechanism of SARS-CoV-2 infection inhibition by ARB. Our results demonstrate that ARB physically binds to the spike (S) viral fusion glycoprotein of SARS-CoV-2 as well as its more virulent variants from the United Kingdom (strain B.1.1.7) and South Africa (strain B.1.351). Using chemoproteomics, we further pinpoint the ARB binding site on the S protein to the S2 membrane fusion domain. We use an infection assay with Moloney murine leukemia virus (MLV) pseudoviruses (PVs) pseudotyped with the S proteins of the Wuhan strain and the new variants to show that this interaction is sufficient for the viral cell entry inhibition by ARB. Finally, our experiments reveal that the ARB interaction leads to a significant destabilization and eventual lysosomal degradation of the S protein in cells. Collectively, our findings place ARB among the more promising drug candidates for COVID-19.

RESULTS AND DISCUSSION

Synthesis and Preliminary Evaluation of the ARB-Derived Photoaffinity Probe 1. We initiated our studies by synthesizing an ARB-derived photoaffinity probe for target identification experiments. Probe **1** was designed to feature a benzophenone and an alkyne to enable ultraviolet (UV)-induced photocrosslinking of **1** to its protein targets[35] and further functionalization of **1** via copper(I)-catalyzed alkyne-azide cycloaddition (CuAAC)[36] for subsequent visualization or enrichment (Figure 1A). Previous medicinal chemistry efforts demonstrated that bulkier substituents in positions 2 and 4 of the indole[37−39] moiety of ARB are tolerated, and the antiviral activity is retained. The synthesis of ARB and the ARB probe **1** is presented in Scheme S1A.

We first evaluated if probe **1** shares its protein targets with ARB. To this end, we performed a gel-based in vitro competitive binding assay using a well-established ARB

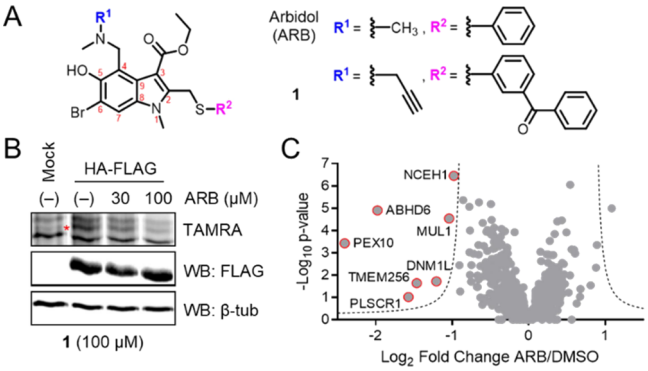

Figure 1. Evaluation of the ARB-derived probe **1** and chemoproteomic profiling of ARB cellular targets. (a) Chemical structures of ARB and the photoaffinity probe **1**. (b) Gel-based competitive profiling of HA-FLAG binding by ARB. HEK293T cell lysates overexpressing HA-FLAG were pretreated with the indicated concentrations of ARB for 1 h, followed by 1 h cotreatment with 100 μM **1** and subsequent 20 min UV irradiation. Shown are the TAMRA fluorescence profile of **1** (top), Western blot membrane probed for FLAG (middle), and β-tubulin (bottom). Asterisk indicates HA-FLAG. (c) Volcano plot showing **1**-enriched and ARB-competed proteins identified via LC−MS/MS-based in situ pulldown from A549 cells. Cells were pretreated with DMSO or 10 μM ARB for 1 h, followed by 4 h cotreatment with 100 μM **1** and subsequent 20 min UV irradiation (n = 6, three biologicals, and two technicals each). Data are represented as $\log_2$ fold change; dotted lines represent a false discovery rate of 5% and an S_0 of 2.

binding partner, the viral fusion protein complex hemagglutinin (HA) from the influenza virus strain A/Puerto Rico/8/1934(H1N1).[40] FLAG-tagged HA overexpressing HEK293T cellular lysates were pretreated with indicated concentrations of ARB for 1 h, followed by 1 h treatment with 100 μM **1** and 20 min UV irradiation on ice. Lysates were then conjugated to tetramethylrhodamine (TAMRA)-azide via CuAAC, separated by sodium dodecyl sulfate−polyacrylamide gel electrophoresis (SDS-PAGE), and scanned for fluorescence (Figure 1B). Indeed, probe **1** labeled HA-FLAG, and the corresponding fluorescent band was competed in a concentration-dependent manner by ARB demonstrating that **1** is a suitable probe for ARB protein target identification.

ARB induces changes in lipid membrane fluidity and cellular trafficking, and it is believed that these changes contribute to the antiviral effects of this drug.[21] Binding of ARB to cellular proteins has been discussed as its potential mechanism of action but has never been explored.[41] Accordingly, we first sought to evaluate if the ARB activity against SARS-CoV-2 could be explained through interactions with the host cell proteome. Following our longstanding interest in bioactive small molecule target identification,[42−44] we performed a competitive pulldown with **1** coupled with liquid chromatography−tandem mass spectrometry (LC−MS/MS) analysis (Figure 1C, S1, Table S1). A549 cells, which are widely used as a model in respiratory virus research,[45−47] were pretreated with 10 μM ARB, based on nontoxic blood plasma levels in patients,[48] or dimethyl sulfoxide (DMSO) for 1 h, then treated with 100 μM **1** for 4 h, UV-irradiated, and lysed. Proteins were conjugated to biotin-azide, enriched over streptavidin beads, digested, and analyzed via LC−MS/MS. Under these conditions, seven targets were significantly competed by ARB. However, none of the seven targets overlapped with the recently reported human protein SARS-CoV-2 interac-

https://doi.org/10.1021/acschembio.1c00756
ACS Chem. Biol. XXXX, XXX, XXX−XXX

tome.[49] Furthermore, literature survey also failed to provide any plausible links between the identified targets and the known machinery involved in viral infection.

ARB Binds to the SARS-CoV-2 S Protein. We next proceeded with the investigation of possible direct interactions between ARB and SARS-CoV-2 proteins. Sequence similarities were recently reported for a region in the trimerization domains of influenza virus (H3N2) HA and SARS-CoV-2 S viral fusion glycoproteins and an in silico docking model proposed ARB binding to the viral S protein, however, without any experimental proof.[50] To assess the ARB selectivity toward the S protein, all three surface proteins of SARS-CoV-2 (the S, the membrane (M), and the small envelope (E) proteins) were screened for **1** binding in a gel-based labeling assay. HEK293T lysates with individually overexpressed S-3xFLAG, M-2xStrep, or E-2xStrep were treated with **1**, followed by TAMRA-azide conjugation and in-gel fluorescence scanning (Figure 2A, S2A). A new fluorescent band was only observed with S-3xFLAG, indicating selective engagement of the S protein by **1** (Figure 2A,B). In contrast, **1** did not label the overexpressed human protein TMPRSS2-FLAG (Figure S2B), thus effectively eliminating the possibility of artifactual S protein labeling via the FLAG-tag. Consequently, we focused on further validation and characterization of the ARB-S protein interaction.

First, we confirmed by chemical pulldown and subsequent Western blotting that **1** binds to the S protein but not the M or the E proteins (Figure 2C). Indeed, we observed that partial competition of S-3xFLAG labeling with 10 μM ARB and pretreatment with 30 μM drug almost completely abolished the labeling. M-2xStrep and E-2xStrep, on the contrary, were not enriched by **1**, indicating no binding. Second, we made use of the thermal shift assay (TSA)[51] to additionally probe ARB interactions with the S protein. HEK293T lysates overexpressing S-3xFLAG were treated with 30 μM ARB or DMSO and subjected to heating at increasing temperatures to cause thermal denaturation and precipitation of proteins. Soluble protein fractions obtained after centrifugation were then probed by Western blotting with an anti-FLAG antibody. We observed a ΔT_m of 7.2 °C, indicating significant thermal destabilization of S-3xFLAG by ARB (Figure 2D, S3A), while the negative control E-2xStrep showed no effect (Figure S3B). Next, we tested by TSA the highly infectious variants of SARS-CoV-2 originating from the United Kingdom (strain B.1.1.7 or "UK") and South Africa (strain B.1.351 or "SA").[13−15] We obtained significant ΔT_{ms} of 6.8 °C and 8.3 °C for the UK and SA variants, respectively, indicating that ARB also binds to the new variants (Figure 2D, S3C). Using a gel-based competitive assay, we measured EC_{50} values of 5.5, 3.2, and 4.6 μM for the binding of ARB to S-3xFLAG, S-FLAG (UK), and S-FLAG (SA), respectively, showing that ARB is an equally potent binder to these emerging S protein variants (Figure 2E, S4). These values are similar to the reported EC_{50} for the ARB inhibition of SARS-CoV-2 infection in cells (4.11 μM)[34] and blood plasma ARB levels in human patients (2.16 mg/L or 4.5 μM).[48] Collectively, our results suggest that ARB interacts with the S protein and destabilizes its structure in situ.

ARB Binds to the S2 Domain Region of the S Protein. Having identified the S protein as the ARB binding partner, we proceeded with the determination of the precise ARB binding site on the S protein. The binding site mapping was carried out using the recently established limited proteolysis-coupled mass spectrometry approach (LiP-MS).[52] Purified S-His protein was incubated with ARB or DMSO for 1 h, and limited proteolysis

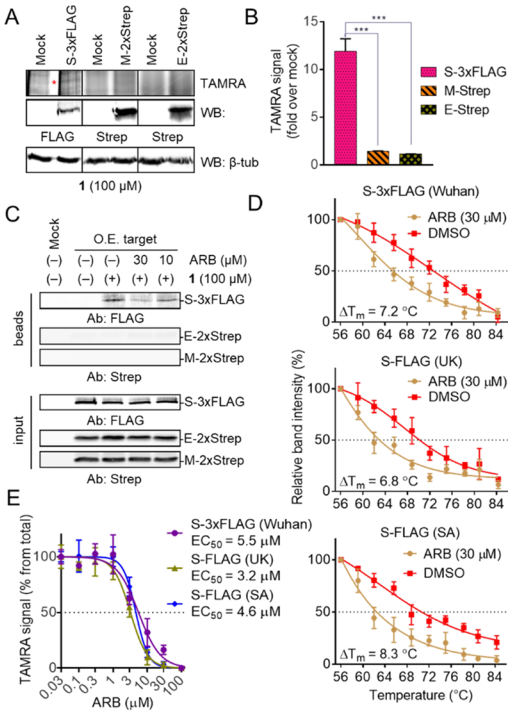

Figure 2. Identification and validation of the SARS-CoV-2 S glycoprotein as an in situ protein target of ARB. (a) Gel-based in vitro screening of **1** binding to SARS-CoV-2 surface proteins. HEK293T cell lysates overexpressing indicated proteins were treated with 100 μM **1** for 1 h, followed by 20 min UV irradiation. Shown are the TAMRA fluorescence profile of **1** (top), Western blot membrane probed for FLAG or Strep (middle), and β-tubulin (bottom). Asterisk indicates the protein band of interest. (b) Quantification of gel-based screening in (a). TAMRA **1** signal increase in overexpressed lanes versus mock was quantified and normalized by target protein expression levels (n = 3, relative values ±SD). ***p < 0.0005 by unpaired Student's t-test. (c) In situ competitive **1** pulldown of indicated proteins, followed by Western blotting. HEK293T cells overexpressing S-3xFLAG, M-2xStrep, or E-2xStrep were pretreated with indicated concentrations of ARB for 1 h, followed by 4 h cotreatment with 100 μM **1** and subsequent 20 min UV irradiation, then lysed. Probe-labeled proteins were conjugated to biotin-azide via CuAAC, enriched using streptavidin beads, eluted, separated by SDS-PAGE, and probed by Western blotting. (d) Thermal destabilization of the S protein from SARS-CoV-2 strains Wuhan, B.1.1.7 "UK", and B.1.351 "SA" by ARB measured by the TSA. HEK293T lysates overexpressing the indicated S protein were treated with 30 μM ARB or DMSO for 1 h, followed by 3 min heat treatment at indicated temperatures. Soluble protein fractions were then transferred on Western blot membranes, probed for FLAG, and bands were quantified (n = 3, relative values ±SD and ΔT_m). (e) EC_{50} values of the ARB-S protein (strains Wuhan, B.1.1.7 "UK", and B.1.351 "SA") interaction calculated using a gel-based competitive in vitro binding assay, as shown in Figure S4 (n = 3, relative values ±SD and EC_{50}).

under native conditions was conducted for 1 min with the broad-spectrum protease proteinase K. Partially digested protein samples were then denatured, fully digested with trypsin overnight, and analyzed by LC−MS/MS. A total of 74 half-tryptic and nontryptic peptides homogeneously covering the whole sequence of S-His were successfully quantified. Out of these 74 detected peptides, only two overlapping non- or half-tryptic peptides, (GYHLMSFPQSAPHGVVFLHVT [aa 1046−1066] and PQSAPHGVVFLHVT [aa 1053−1066]), were found to be significantly protected by ARB (Figure 3A,

https://doi.org/10.1021/acschembio.1c00756
ACS Chem. Biol. XXXX, XXX, XXX−XXX

A

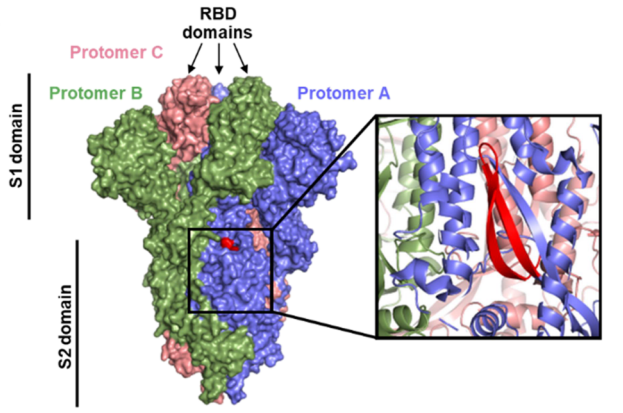

B

S-3xFLAG Mutation	WT	S1021A	L1024A	T1027A	F1062A	L1063A	H1064A
ΔTm	7.2 °C	5.3 °C	4.7 °C	2.7 °C	4.3 °C	6.4 °C	2.6 °C
ΔTm_{WT}-ΔTm_{MUT}		1.9 °C	2.5 °C	4.5 °C	2.9 °C	0.8 °C	4.6 °C

Figure 3. ARB binds to the S2 domain region of the S protein. (a) ARB binding site identified via LiP-MS (n = 6, 3 biologicals and 2 technicals) was mapped into the surface representation of the cryo-EM structure of SARS-CoV-2 S protein (pdb: 6vxx). Protomers A, B, and C are shown in blue, green, and pink, respectively. ARB binding site [aa 1046−1066] is shown in red. Window on the right represents a magnified cartoon representation of the ARB-binding protein region. (b) Results of TSA experiments comparing the thermal destabilization of indicated overexpressed S-3xFLAG mutants to the wild-type protein upon 30 μM ARB treatment in HEK293T lysates. ΔTm indicates the thermal shift in ARB- vs DMSO-treated samples. $\Delta T_{mWT} - \Delta T_{mMUT}$ indicates the thermal shift difference between the indicated S-3xFLAG mutant and the wild-type protein. Corresponding Western blots and individual graphs are presented in Figure 2D, S3A, S8.

S5, Table S2). This region [1046−1066] is located in close vicinity to the trimerization interface in the S2 membrane fusion domain and consists of two antiparallel β-strands. The discovered ARB binding region is located distantly from the mutation sites in the S protein of SARS-CoV-2 UK and SA variants, which may explain why ARB also binds to the mutant S proteins (Figure 2E, S4). Importantly, our ARB binding site identified by LiP-MS is also part of the ARB binding region predicted in silico by molecular docking.[50] Cell membrane adhesion and endosomal internalization of SARS-CoV-2 is mediated through the interaction of the S protein receptor-binding domain (RBD) and the extracellular portion of its human cell entry receptor angiotensin-converting enzyme 2 (ACE2).[53−56] As expected, neither RBD-His nor sACE2-His (a soluble extracellular portion of ACE2) overexpressed in HEK293T lysates was labeled by **1** in a gel-based assay, additionally confirming that ARB neither binds to the ACE2-interacting RBD domain of the S protein nor to the ACE2 receptor (Figure S6).

Next, we generated single-site alanine substitution S-3xFLAG mutants for the selected amino acid positions of the target peptide 1046−1066 (F1062A, L1063A, and H1064A) and the neighboring alpha helix (S1021, L1024A, T1027A), together forming the proposed ARB-binding cavity on the S protein trimerization interface (Figure S7). The impact of ARB treatment on thermal stability was then compared between the mutant and the wild-type S-3xFLAG proteins overexpressed in HEK293T lysates using TSA (Figure 2D and Figure 3B, S3A, S8). The S1021A, L1024A, and F1062A (ΔT_{ms} of 5.3, 4.7, 4.3 °C, respectively) and, most notably, the T1027A and H1064A mutants (ΔT_{ms} of 2.7 and 2.6 °C, respectively) exhibited decreased thermal destabilization by ARB compared to the wild-type protein (ΔT_m: 7.2 °C), corresponding to a decrease in their ARB binding affinity. The negative control mutant L1063A (ΔT_m: 6.4 °C), on the other hand, showed conserved ARB binding with no significant difference from the wild type. The side chain of the residue L1063 points outward of the proposed ARB-binding cavity, while the side chains of the residues S1021, L1024, T1027, F1062, and H1064 all point toward it (Figure S7).

ARB Inhibits SARS-CoV-2 Entry through Interaction with the S Protein. Previous reports showed that ARB exhibits its antiviral effects against influenza and HCV via both protein and lipid membrane interactions.[21] Hence, we hypothesized that ARB analogues that structurally closely resemble ARB but show reduced S protein binding affinity would serve as important controls to further confirm the ARB mode of action. Compared to ARB, compound **2** misses the dimethylaminomethane substituent in position 4 of the indole. Compound **3** lacks both the bromide substituent in position 6 and the thiophenyl group on the 2-methyl substituent (Figure 4A, Scheme S1). We pretreated S-His with DMSO, ARB, **2**, or **3**, followed by **1** and measured the remaining signal of **1**-labeled S-His by in-gel fluorescence scanning (Figure 4B, S9A). The S-His fluorescence band was not competed by **2** or **3** at concentrations up to 100 μM, while ARB, as expected, showed significant competition at 30 μM concentration. This experiment successfully established **2** and **3** as inactive ARB analogues and highlighted the importance of amine in position 4.

Next, we sought to evaluate the effect of ARB and analogues on viral entry in mammalian cells. MLV-based pseudoviruses (PVs), encoding firefly luciferase and pseudotyped with the S protein of SARS-CoV-2 strains Wuhan, UK, or SA were produced from transfected HEK293T cells, as previously described.[57] PVs were incubated with ARB, **2**, **3**, or DMSO for 1 h, then added to HEK293T cells stably overexpressing human SARS-CoV-2 cell entry receptor angiotensin-converting enzyme 2 (hACE2-293T),[53−56] and removed after 3 h. Cells were lysed 24 h postinfection, and luciferase activity was measured and used as a readout for PV cell entry. Indeed, ARB efficiently inhibited the cell entry of PVs carrying the S protein of all three tested variants, Wuhan, UK, and SA, with an EC_{50} of ∼5 μM (Figure 4C). These EC_{50}s are in good accordance with our measured ARB binding to the S protein variants (Figure 2E, S4) and the reported EC_{50} of SARS-CoV-2 cell entry inhibition (4.11 μM).[34] In contrast, neither **2** nor **3** showed a significant effect at concentrations up to 30 μM (Figure 4C). Importantly, adding ARB to both hACE2-293T cells and PVs versus PVs alone did not improve the PV cell entry inhibition, further confirming that the anti-SARS-CoV-2 effect of ARB originates from the direct interaction with the S protein rather than binding to the cellular targets (Figure S9B). These data collectively suggest that binding of ARB to the S protein is both required and sufficient for the inhibition of SARS-CoV-2 human cell entry.

ARB Induces Lysosomal Degradation of the S Protein. ARB incubation with S protein-overexpressing lysates caused strong thermal destabilization of the S protein (Figure 2D, S3A, S3C). We therefore speculated whether ARB might

https://doi.org/10.1021/acschembio.1c00756
ACS Chem. Biol. XXXX, XXX, XXX−XXX

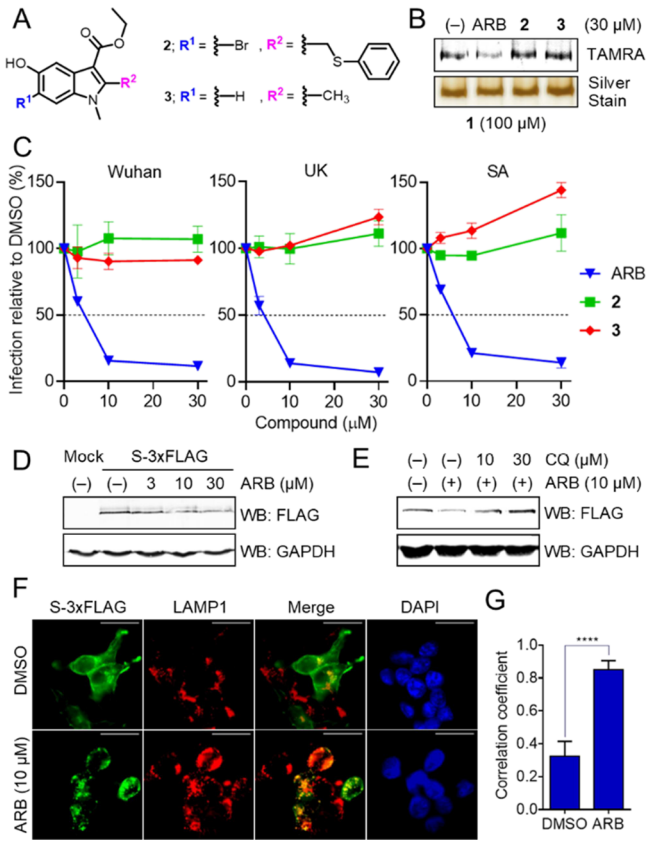

Figure 4. ARB inhibits the cell entry of S protein-pseudotyped MLV viruses and leads to the lysosomal degradation of the S protein. (a) Chemical structures of inactive ARB analogues **2** and **3**. (b) Gel-based in vitro competitive assay comparing purified S-His binding activity of ARB and analogues. S-His was pretreated with 30 μM of indicated compounds for 1 h, followed by 1 h cotreatment with 100 μM **1** and subsequent 20 min UV irradiation. Shown is the TAMRA fluorescence profile of **1** and silver staining. (c) Effect of ARB and analogues on MLV PV infection. MLV PVs pseudotyped with the S protein from the strains Wuhan, B.1.1.7 "UK", or B.1.351 "SA" were pretreated with compounds at indicated concentrations for 1 h and then incubated with hACE2 overexpressing HEK293T cells for 3 h. Cells were lysed 24 h after infection, and lysates were probed for luciferase activity (n = 3, relative values ± SD). (d) Western blot showing ARB concentration-dependent degradation of S-3xFLAG (top) and glyceraldehyde-3-phosphate dehydrogenase (GAPDH) control (bottom). (e) Western blot showing ARB-induced S-3xFLAG degradation and degradation rescue upon chloroquine (CQ) treatment (top) and GAPDH control (bottom). S-3xFLAG overexpressing HEK293T cells were treated with 10 μM ARB together with indicated concentrations of CQ for 16 h. (f) Fluorescence microscopy images of S-3xFLAG-overexpressing HEK293T cells upon 16 h treatment with DMSO or 10 μM ARB. FLAG, LAMP1, and DAPI stains are shown in green, red, and blue, respectively. Scale bars indicate 30 μm. (g) Quantification of S-3xFLAG/LAMP1 colocalization from the microscopy experiment in (f). Colocalization is described by the computed average of the Pearson's correlation coefficient ($n \geq 30$ cells). Error bars are SD. ****$p < 0.0001$ by unpaired Student's t-test.

be causing structural changes such as unfolding, precipitation, or aggregation of the S protein that could also lead to a decreased stability of this protein in cells. When we treated the S-3xFLAG-overexpressing HEK293T cells with ARB for 16 h, Western blotting revealed concentration-dependent decrease in the S-3xFLAG expression levels (Figure 4D). We hypothesized that one of the two major mammalian protein degradation pathways,[58] the ubiquitin–proteasome system (UPS) or the autophagy–lysosome pathway (ALP), could be responsible for ARB-induced S protein degradation. To investigate this hypothesis, S-3xFLAG-overexpressing HEK293T cells were cotreated with 10 μM ARB and increasing concentrations of chloroquine (CQ), an ALP inhibitor, or MG132, an UPS inhibitor, for 16 h, then lysed and probed for S-3xFLAG expression by Western blotting (Figure 4E, S9C). Indeed, CQ cotreatment resulted in the concentration-dependent rescue of S-3xFLAG expression levels, while MG132 showed no effect on ARB-induced S-3xFLAG proteolysis, suggesting that degradation is likely mediated through ALP. Additionally, we performed fluorescence microscopy experiments with S-3xFLAG-overexpressing HEK293T cells to monitor the protein localization changes upon ARB treatment. Cells were treated with ARB or DMSO for 16 h, fixed, and immunostained for S-3xFLAG and lysosomal-associated membrane protein 1 (LAMP1, Figure 4F). Indeed, we observed a significant increase in S-3xFLAG colocalization with the lysosomal marker LAMP1 in ARB- versus DMSO-treated cells (Figure 4G). This illustrates that S-3xFLAG localizes to lysosomes, following an interaction with ARB. Even though further in situ validation with native SARS-CoV-2 is clearly needed, ARB-induced lysosomal degradation of the S protein could be causing a decrease in functional titers of the de novo-synthesized viral particles as part of the late-stage (postentry) therapeutic effect of ARB.

CONCLUSIONS

In summary, our study provides the molecular mechanism of the therapeutic effect of ARB against SARS-CoV-2. We show that ARB directly binds to the SARS-CoV-2 protein S, locate its binding site in the S2 membrane fusion domain, and discover the essential structural elements of ARB that govern the binding. We further demonstrate that this interaction is the driver for the viral cell entry inhibition by ARB, ultimately resulting in the lysosomal degradation of the viral S protein. Our results therefore establish ARB as a direct-acting anti-SARS-CoV-2 agent. The example of ARB also demonstrates that the S protein is druggable by therapeutic small molecules, as opposed to commonly exploited peptides and antibodies.

Most importantly, our study reveals that ARB is also capable of binding and inhibiting the cell entry of the mutant S protein-presenting pseudoviruses originating from the quickly propagating and more virulent variants of SARS-CoV-2 from the United Kingdom (strain B.1.1.7) and South Africa (strain B.1.351), two strains that display increased resistance to neutralizing antibodies and vaccines and currently represent a global health concern, causing a new wave of lockdown and strengthening travel restrictions.[11−15]

Together with the early clinical data, we believe that our findings place ARB among the more promising drug candidates for COVID-19. Because of the tremendous time pressure created by the ongoing pandemic, almost 30 years of clinical history in Russia and China yield ARB a significant advantage over the newly developed drug candidates and may therefore create a possible route to expedited approval in the Western countries.

https://doi.org/10.1021/acschembio.1c00756
ACS Chem. Biol. XXXX, XXX, XXX−XXX

■ ASSOCIATED CONTENT

Supporting Information

The Supporting Information is available free of charge at https://pubs.acs.org/doi/10.1021/acschembio.1c00756.

Experimental procedures, supplemental figures, supplemental tables, and NMR spectra (PDF)

■ AUTHOR INFORMATION

Corresponding Author

Alexander Adibekian − *Department of Chemistry, The Scripps Research Institute, Jupiter, Florida 33458, United States;* orcid.org/0000-0001-6453-0244; Email: aadibeki@scripps.edu

Authors

Anton Shuster − *Department of Chemistry, The Scripps Research Institute, Jupiter, Florida 33458, United States*

Dany Pechalrieu − *Department of Chemistry, The Scripps Research Institute, Jupiter, Florida 33458, United States*

Cody B Jackson − *Department of Immunology and Microbiology, The Scripps Research Institute, Jupiter, Florida 33458, United States*

Daniel Abegg − *Department of Chemistry, The Scripps Research Institute, Jupiter, Florida 33458, United States*

Hyeryun Choe − *Department of Immunology and Microbiology, The Scripps Research Institute, Jupiter, Florida 33458, United States*

Complete contact information is available at: https://pubs.acs.org/10.1021/acschembio.1c00756

Author Contributions

§A.S. and D.P. contributed equally

Funding

Administrative supplement to NIH R01 AI129868 for coronavirus research (H.C.)

Notes

The authors declare no competing financial interest.

■ ACKNOWLEDGMENTS

We thank The Scripps Research Institute and the administrative supplement to NIH R01 AI129868 for coronavirus research (H.C.) for financial support. We thank B. Quinlan and the Farzan lab for kindly providing the expression vectors for the S protein strains B.1.1.7 "UK" and B.1.351 "SA."

■ REFERENCES

(1) Guo, G.; Ye, L.; Pan, K.; Chen, Y.; Xing, D.; Yan, K.; Chen, Z.; Ding, N.; Li, W.; Huang, H.; Zhang, L.; Li, X.; Xue, X. New Insights of Emerging SARS-CoV-2: Epidemiology, Etiology, Clinical Features, Clinical Treatment, and Prevention. *Front. Cell Dev. Biol.* **2020**, *8*, 410.

(2) Petersen, E.; Koopmans, M.; Go, U.; Hamer, D. H.; Petrosillo, N.; Castelli, F.; Storgaard, M.; Al Khalili, S.; Simonsen, L. Comparing SARS-CoV-2 with SARS-CoV and Influenza Pandemics. *Lancet Infect. Dis.* **2020**, *20*, No. e238.

(3) Feng, W.; Zong, W.; Wang, F.; Ju, S. Severe Acute Respiratory Syndrome Coronavirus 2 (SARS-CoV-2): A Review. *Mol. Cancer* **2020**, *19*, 100.

(4) World Health Organisation [WHO]. Weekly epidemiological update. Feb. 09; **2021** https://www.who.int/publications/m/item/weekly-epidemiological-update---9-february-2021.

(5) Lamb, Y. N. Remdesivir: First Approval. *Drugs* **2020**, *80*, 1355−1363.

(6) Beigel, J. H.; Tomashek, K. M.; Dodd, L. E.; Mehta, A. K.; Zingman, B. S.; Kalil, A. C.; Hohmann, E.; Chu, H. Y.; Luetkemeyer, A.; Kline, S.; Lopez de Castilla, D.; Finberg, R. W.; Dierberg, K.; Tapson, V.; Hsieh, L.; Patterson, T. F.; Paredes, R.; Sweeney, D. A.; Short, W. R.; Touloumi, G.; Lye, D. C.; Ohmagari, N.; Oh, M. D.; Ruiz-Palacios, G. M.; Benfield, T.; Fätkenheuer, G.; Kortepeter, M. G.; Atmar, R. L.; Creech, C. B.; Lundgren, J.; Babiker, A. G.; Pett, S.; Neaton, J. D.; Burgess, T. H.; Bonnett, T.; Green, M.; Makowski, M.; Osinusi, A.; Nayak, S.; Lane, H. C. Remdesivir for the Treatment of Covid-19 — Final Report. *N Engl J Med* **2020**, *383*, 1813.

(7) Lloyd, E. C.; Gandhi, T. N.; Petty, L. A. Monoclonal Antibodies for COVID-19. *JAMA* **2021**, *325*, 1015.

(8) Cohen, M. S. Monoclonal Antibodies to Disrupt Progression of Early Covid-19 Infection. *N. Engl. J. Med.* **2021**, *384*, 289−291.

(9) Eli Lilly and Company. *A Randomized, Double-Blind, Placebo-Controlled, Phase 2/3 Study to Evaluate the Efficacy and Safety of LY3819253 and LY3832479 in Participants With Mild to Moderate COVID-19 Illness*; Clinical trial registration NCT04427501; clinicaltrials.gov, 2021.

(10) Forni, G.; Mantovani, A. COVID-19 Vaccines: Where We Stand and Challenges Ahead. *Cell Death Differ.* **2021**, *28*, 626−639.

(11) Tegally, H.; Wilkinson, E.; Giovanetti, M.; Iranzadeh, A.; Fonseca, V.; Giandhari, J.; Doolabh, D.; Pillay, S.; San, E. J.; Msomi, N. Emergence and Rapid Spread of a New Severe Acute Respiratory Syndrome-Related Coronavirus 2 (SARS-CoV-2) Lineage with Multiple Spike Mutations in South Africa. *med Rxiv* **2020**, No. 248640.

(12) Santos, J. C.; Passos, G. A. The High Infectivity of SARS-CoV-2 B.1.1.7 Is Associated with Increased Interaction Force between Spike-ACE2 Caused by the Viral N501Y Mutation. *bio Rxiv* **2021**, No. 424708.

(13) Wang, P.; Liu, L.; Iketani, S.; Luo, Y.; Guo, Y.; Wang, M.; Yu, J.; Zhang, B.; Kwong, P. D.; Graham, B. S. Increased Resistance of SARS-CoV-2 Variants B.1.351 and B.1.1.7 to Antibody Neutralization. *bio Rxiv* **2021**, No. 428137.

(14) Collier, D. A.; Marco, A. D.; Ferreira, I. A. T. M.; Meng, B.; Datir, R.; Walls, A. C.; Bassi, J.; Pinto, D. SARS-CoV-2 B.1.1.7 Escape from MRNA Vaccine-Elicited Neutralizing Antibodies. *med Rxiv* **2021**, No. 21249840.

(15) Schnirring, L. New variant COVID findings fuel more worries about vaccine resistance. Feb. 02; 2021. https://www.cidrap.umn.edu/news-perspective/2021/02/new-variant-covid-findings-fuel-more-worries-about-vaccine-resistance.

(16) Kupferschmidt, K.; Cohen, J..; 2020; Pm, 3: 28. WHO launches global megatrial of the four most promising coronavirus treatments https://www.sciencemag.org/news/2020/03/who-launches-global-megatrial-four-most-promising-coronavirus-treatments.

(17) World Health Organisation [WHO]. *Coronovirus (COVID-19) Update No. 22 The Solidarity Trial.* Apr. 16; 2020.

(18) National Institutes of Health [NIH]. NIH to Launch Public-Private Partnership to Speed COVID-19 Vaccine and Treatment Options. Apr 17; 2020.

(19) Fragkou, P. C.; Belhadi, D.; Peiffer-Smadja, N.; Moschopoulos, C. D.; Lescure, F.-X.; Janocha, H.; Karofylakis, E.; Yazdanpanah, Y.; Mentré, F.; Skevaki, C.; Laouénan, C.; Tsiodras, S. Review of Trials Currently Testing Treatment and Prevention of COVID-19. *Clin. Microbiol. Infect.* **2020**, *26*, 988−998.

(20) Liu, M.-Y.; Wang, S.; Yao, W.-F.; Wu, H.; Meng, S.-N.; Wei, M.-J. Pharmacokinetic Properties and Bioequivalence of Two Formulations of Arbidol: An Open-Label, Single-Dose, Randomized-Sequence, Two-Period Crossover Study in Healthy Chinese Male Volunteers. *Clin. Ther.* **2009**, *31*, 784−792.

(21) Blaising, J.; Polyak, S. J.; Pécheur, E.-I. Arbidol as a Broad-Spectrum Antiviral: An Update. *Antiviral Res.* **2014**, *107*, 84−94.

(22) Boriskin, Y. S.; Leneva, I. A.; Pécheur, E.-I.; Polyak, S. J. Arbidol: A Broad-Spectrum Antiviral Compound That Blocks Viral Fusion. *Curr. Med. Chem.* **2008**, *15*, 997−1005.

(23) Oestereich, L.; Rieger, T.; Neumann, M.; Bernreuther, C.; Lehmann, M.; Krasemann, S.; Wurr, S.; Emmerich, P.; de Lamballerie,

X.; Ölschläger, S.; Günther, S. Evaluation of Antiviral Efficacy of Ribavirin, Arbidol, and T-705 (Favipiravir) in a Mouse Model for Crimean-Congo Hemorrhagic Fever. *PLoS Negl. Trop. Dis.* **2014**, *8*, No. e2804.
(24) Perfetto, B.; Filosa, R.; De Gregorio, V.; Peduto, A.; La Gatta, A.; de Caprariis, P.; Tufano, M. A.; Donnarumma, G. In Vitro Antiviral and Immunomodulatory Activity of Arbidol and Structurally Related Derivatives in Herpes Simplex Virus Type 1-Infected Human Keratinocytes (HaCat). *J. Med. Microbiol.* **2014**, *63*, 1474−1483.
(25) Hulseberg, C. E.; Fénéant, L.; Szymańska-de Wij, K. M.; Kessler, N. P.; Nelson, E. A.; Shoemaker, C. J.; Schmaljohn, C. S.; Polyak, S. J.; White, J. M. Arbidol and Other Low-Molecular-Weight Drugs That Inhibit Lassa and Ebola Viruses. *J. Virol.* **2019**, *93* (8), No. e02185-18.
(26) Du, Q.; Gu, Z.; Leneva, I.; Jiang, H.; Li, R.; Deng, L.; Yang, Z. The Antiviral Activity of Arbidol Hydrochloride against Herpes Simplex Virus Type II (HSV-2) in a Mouse Model of Vaginitis. *Int. Immunopharmacol.* **2019**, *68*, 58−67.
(27) Glushkov, R.G.; Maksimov, V.A.; Mart'janov, V.A.; Khamitov, R.A.; Shuster, A.M. *Medicinal agent for treatment of atypical pneumonia, RU 2 256 451 C1*; Federal Service for Intellectual Property, Patents and Trademarks, Russian Federation, April 21, 2004.
(28) Khamitov, R. A.; Loginova, S. I.; Shchukina, V. N.; Borisevich, S. V.; Maksimov, V. A.; Shuster, A. M. Antiviral activity of arbidol and its derivatives against the pathogen of severe acute respiratory syndrome in the cell cultures. *Vopr. Virusol.* **2008**, *53*, 9−13.
(29) Shuster, A. M.; Ya, S. L.; Schukina, V. N.; Borisevich, S. V.; Khamitov, R. A.; Maksimov, V. A. Analysis of Arbidol® Efficiency against an Experimental Form of Severe Acute Respiratory Syndrome. *Antibiot. Chemother. RU* **2019**, *64*, 1.
(30) Zhang, J.; Zhou, L.; Yang, Y.; Peng, W.; Wang, W.; Chen, X. Therapeutic and Triage Strategies for 2019 Novel Coronavirus Disease in Fever Clinics. *Lancet Respir. Med.* **2020**, *8*, e11−e12.
(31) Deng, L.; Li, C.; Zeng, Q.; Liu, X.; Li, X.; Zhang, H.; Hong, Z.; Xia, J. Arbidol Combined with LPV/r versus LPV/r Alone against Corona Virus Disease 2019: A Retrospective Cohort Study. *J. Infect.* **2020**, *81*, e1−e5.
(32) Zhu, Z.; Lu, Z.; Xu, T.; Chen, C.; Yang, G.; Zha, T.; Lu, J.; Xue, Y. Arbidol Monotherapy Is Superior to Lopinavir/Ritonavir in Treating COVID-19. *J. Infect.* **2020**, *81*, e21−e23.
(33) Wang, Z.; Yang, B.; Li, Q.; Wen, L.; Zhang, R. Clinical Features of 69 Cases With Coronavirus Disease 2019 in Wuhan. *China. Clin. Infect. Dis.* **2020**, *71*, 769−777.
(34) Wang, X.; Cao, R.; Zhang, H.; Liu, J.; Xu, M.; Hu, H.; Li, Y.; Zhao, L.; Li, W.; Sun, X.; et al. The Anti-Influenza Virus Drug, Arbidol Is an Efficient Inhibitor of SARS-CoV-2 in Vitro. *Cell Discov.* **2020**, *6*, 28.
(35) Dormán, G.; Nakamura, H.; Pulsipher, A.; Prestwich, G. D. The Life of Pi Star: Exploring the Exciting and Forbidden Worlds of the Benzophenone Photophore. *Chem. Rev.* **2016**, *116*, 15284−15398.
(36) Speers, A. E.; Cravatt, B. F. Profiling Enzyme Activities In Vivo Using Click Chemistry Methods. *Chem. Biol.* **2004**, *11*, 535−546.
(37) Zotova, S. A.; Korneeva, T. M.; Shvedov, V. I.; Fadeeva, N. I.; Leneva, I. A.; Fedyakina, I. T.; Khristova, M. L.; Nikolaeva, I. S.; Peters, V. V.; Gus'kova, T. A. Synthesis and Antiviral Activity of Indole and Benzofuran Sulfides. *Pharm. Chem. J.* **1995**, *29*, 57−59.
(38) Ivashchenko, A. V.; Yamanushkin, P. M.; Mit'kin, O. D.; Kisil', V. M.; Korzinov, O. M.; Vedenskii, V. Y.; Leneva, I. A.; Bulanova, E. A.; Bychko, V. V.; Okun', I. M. Synthesis and Antiviral Activity of Ethyl 1, 2-Dimethyl-5-Hydroxy-1H-Indole-3-Carboxylates and Their Derivatives. *Pharm. Chem. J.* **2014**, *47*, 636−650.
(39) Wright, Z. V. F.; Wu, N. C.; Kadam, R. U.; Wilson, I. A.; Wolan, D. W. Structure-Based Optimization and Synthesis of Antiviral Drug Arbidol Analogues with Significantly Improved Affinity to Influenza Hemagglutinin. *Bioorg. Med. Chem. Lett.* **2017**, *27*, 3744−3748.
(40) Kadam, R. U.; Wilson, I. A. Structural Basis of Influenza Virus Fusion Inhibition by the Antiviral Drug Arbidol. *Proc. Natl. Acad. Sci.* **2017**, *114*, 206−214.
(41) Blaising, J.; Lévy, P. L.; Polyak, S. J.; Stanifer, M.; Boulant, S.; Pécheur, E.-I. Arbidol Inhibits Viral Entry by Interfering with Clathrin-Dependent Trafficking. *Antiviral Res.* **2013**, *100*, 215−219.
(42) Abegg, D.; Frei, R.; Cerato, L.; Prasad Hari, D.; Wang, C.; Waser, J.; Adibekian, A. Proteome-Wide Profiling of Targets of Cysteine Reactive Small Molecules by Using Ethynyl Benziodoxolone Reagents. *Angew. Chem., Int. Ed.* **2015**, *54*, 10852−10857.
(43) Wang, C.; Abegg, D.; Hoch, D. G.; Adibekian, A. Chemoproteomics-Enabled Discovery of a Potent and Selective Inhibitor of the DNA Repair Protein MGMT. *Angew. Chem., Int. Ed.* **2016**, *55*, 2911−2915.
(44) Hoch, D. G.; Abegg, D.; Hannich, J. T.; Pechalrieu, D.; Shuster, A.; Dwyer, B. G.; Wang, C.; Zhang, X.; You, Q.; Riezman, H.; Adibekian, A. Combined Omics Approach Identifies Gambogic Acid and Related Xanthones as Covalent Inhibitors of the Serine Palmitoyltransferase Complex. *Cell Chem. Biol.* **2020**, *27*, 586−597.e12.
(45) Voigt, E. A.; Swick, A.; Yin, J. Rapid Induction and Persistence of Paracrine-Induced Cellular Antiviral States Arrest Viral Infection Spread in A549 Cells. *Virology* **2016**, *496*, 59−66.
(46) Saleh, F.; Harb, A.; Soudani, N.; Zaraket, H. A Three-Dimensional A549 Cell Culture Model to Study Respiratory Syncytial Virus Infections. *J. Infect. Public Health* **2020**, *13*, 1142−1147.
(47) Rivera-Bahena, G. B.; Márquez-Bandala, A. H.; López-Guerrero, D. V.; Esquivel-Guadarrama, F. R.; Montiel-Hernández, J.-L. TGF-B1 Signaling Inhibit the in Vitro Apoptotic, Infection and Stimulatory Cell Response Induced by Influenza H1N1 Virus Infection on A549 Cells. *Virus Res.* **2021**, *297*, No. 198337.
(48) Sun, Y.; He, X.; Qiu, F.; Zhu, X.; Zhao, M.; Li-Ling, J.; Su, X.; Zhao, L. Pharmacokinetics of Single and Multiple Oral Doses of Arbidol in Healthy Chinese Volunteers. *Int J. Clin. Pharmacol. Ther.* **2013**, *51*, 423−432.
(49) Gordon, D. E.; Jang, G. M.; Bouhaddou, M.; Xu, J.; Obernier, K.; White, K. M.; O'Meara, M. J.; Rezelj, V. V.; Guo, J. Z.; Swaney, D. L. A SARS-CoV-2 Protein Interaction Map Reveals Targets for Drug Repurposing. *Nature* **2020**, *583*, 459−468.
(50) Vankadari, N. Arbidol: A Potential Antiviral Drug for the Treatment of SARS-CoV-2 by Blocking Trimerization of the Spike Glycoprotein. *Int. J. Antimicrob. Agents* **2020**, *56*, No. 105998.
(51) Jafari, R.; Almqvist, H.; Axelsson, H.; Ignatushchenko, M.; Lundbäck, T.; Nordlund, P.; Molina, D. M. The Cellular Thermal Shift Assay for Evaluating Drug Target Interactions in Cells. *Nat. Protoc.* **2014**, *9*, 2100−2122.
(52) Feng, Y.; De Franceschi, G.; Kahraman, A.; Soste, M.; Melnik, A.; Boersema, P. J.; de Laureto, P. P.; Nikolaev, Y.; Oliveira, A. P.; Picotti, P. Global Analysis of Protein Structural Changes in Complex Proteomes. *Nat. Biotechnol.* **2014**, *32*, 1036−1044.
(53) Walls, A. C.; Park, Y.-J.; Tortorici, M. A.; Wall, A.; McGuire, A. T.; Veesler, D. Structure, Function, and Antigenicity of the SARS-CoV-2 Spike Glycoprotein. *Cell* **2020**, *181*, 281−292.e6.
(54) Shang, J.; Ye, G.; Shi, K.; Wan, Y.; Luo, C.; Aihara, H.; Geng, Q.; Auerbach, A.; Li, F. Structural Basis of Receptor Recognition by SARS-CoV-2. *Nature* **2020**, *581*, 221−224.
(55) Ou, X.; Liu, Y.; Lei, X.; Li, P.; Mi, D.; Ren, L.; Guo, L.; Guo, R.; Chen, T.; Hu, J. Characterization of Spike Glycoprotein of SARS-CoV-2 on Virus Entry and Its Immune Cross-Reactivity with SARS-CoV. *Nat. Commun.* **2020**, *11*, 1620.
(56) Shang, J.; Wan, Y.; Luo, C.; Ye, G.; Geng, Q.; Auerbach, A.; Li, F. Cell Entry Mechanisms of SARS-CoV-2. *Proc. Natl. Acad. Sci.* **2020**, *117*, 11727−11734.
(57) Zhang, L.; Jackson, C. B.; Mou, H.; Ojha, A.; Peng, H.; Quinlan, B. D.; Rangarajan, E. S.; Pan, A.; Vanderheiden, A.; Suthar, M. S.; et al. SARS-CoV-2 Spike-Protein D614G Mutation Increases Virion Spike Density and Infectivity. *Nat. Commun.* **2020**, *11*, 6013.
(58) Dikic, I. Proteasomal and Autophagic Degradation Systems. *Annu. Rev. Biochem.* **2017**, *86*, 193−224.

https://doi.org/10.1021/acschembio.1c00756
ACS Chem. Biol. XXXX, XXX, XXX−XXX